Biophys Rev (2017) 9:589–600
DOI 10.1007/s12551-017-0297-z

REVIEW

The many faces (and phases) of ceramide and sphingomyelin I – single lipids

María Laura Fanani[1] · **Bruno Maggio**[1]

Received: 26 May 2017 / Accepted: 27 July 2017 / Published online: 16 August 2017

Abstract Ceramides, the simplest kind of two-chained sphingolipids, contain a single hydroxyl group in position 1 of the sphingoid base. Sphingomyelins further contain a phosphocholine group at the OH of position 1 of ceramide. Ceramides and sphingomyelins show a variety of species depending on the fatty acyl chain length, hydroxylation, and unsaturation. Because of the relatively high transition temperature of sphingomyelin compared to lecithin and, particularly, of ceramides with 16:0–18:0 saturated chains, a widespread idea on their functional importance refers to formation of rather solid domains enriched in sphingomyelin and ceramide. Frequently, and especially in the cell biology field, these are generally (and erroneously) assumed to occur irrespective on the type of N-acyl chain in these lipids. This is because most studies indicating such condensed ordered domains employed sphingolipids with acyl chains with 16 carbons while scarce attention has been focused on the influence of the N-acyl chain on their surface properties. However, abundant evidence has shown that variations of the N-acyl chain length in ceramides and sphingomyelins markedly affect their phase state, interfacial elasticity, surface topography, electrostatics and miscibility and that, even the usually conceived "condensed" sphingolipids and many of their mixtures, may exhibit liquid-like expanded states. This review is a summarized overview of our work and of related others on some facts regarding membranes composed of single molecular species of ceramide and sphingomyelin. A second part is dedicated to discuss the miscibility properties between species of sphingolipids that differ in N-acyl and oligosaccharide chains.

Keywords Lipid domains · Langmuir films · Surface potential · Compressibility modulus · Brewster angle microscopy

This article is part of a Special Issue on 'Latin America' edited by Pietro Ciancaglini and Rosangela Itri

✉ María Laura Fanani
lfanani@fcq.unc.edu.ar

[1] Centro de Investigaciones en Química Biológica de Córdoba (CIQUIBIC-CONICET), Departamento de Química Biológica Ranwel Caputto, Facultad de Ciencias Químicas, Universidad Nacional de Córdoba, Haya de la Torre y Medina Allende, Ciudad Universitaria, X5000HUA, Córdoba, Argentina

Introduction

Sphingolipids comprise a vast family of members constituted by a long-chain aminediol base N-linked to a fatty acid through an amide bond. The importance of these lipids in the plasma membrane and in the organelle endomembranes of eukaryotic cells is not only structural but also functional as lipid mediators in a variety of cellular events. Several sphingolipids, and their metabolically phosphorylated and glycosylated derivatives, have been implicated in membrane signal transduction events, such as biorecognition, differentiation, tumorigenesis, apoptosis, neuroimmunology, and neural regeneration/degeneration of nerve cells (Hakomori 1990). The vast chemical diversity of sphingolipids brought about by independent combination of hydrophobic and hydrophilic moieties leads to an enormous number of structural possibilities (Stults et al. 1989; Maggio et al. 2004). Since the local chemical variations are transduced to different biophysical properties that determine the supramolecular structural dynamics, the variety of membrane effects is further amplified (Maggio et al. 2008; Goñi and Alonso 2009).

The base most usually found, the 18 carbon sphingosine with a trans double bond at position 4–5, is a bioactive lipid

itself, but there are other variants with shorter or longer hydrocarbon chains with different hydroxylation levels and saturation (Hannun and Bell 1989; Maggio 1994; Koynova and Caffrey 1995; Maggio et al. 2004, 2008; Goñi and Alonso 2006; Peñalva et al. 2014a). In addition, the acyl chain linked to the sphingoid base can vary in length, hydroxylation and unsaturation, although long saturated fatty acyl residues are more often encountered in natural sphingolipids than in glycerol-based lipids conferring largely different molecular packing and phase state (Peñalva et al. 2014a). A great variety of polar groups attached to the hydroxyl group at position C1 gives rise to the different families of sphingolipids: among others, ceramides, with a single hydroxyl group; sphingomyelins, with phosphorylcholine (see Scheme 1); cerebrosides and neutral glycosphingolipids with different carbohydrates; and gangliosides with carbohydrates and sialosyl residues (Maggio et al. 1978, 2006).

Sphingomyelin (SM) is the major sphingolipid present in the outer leaflet of cell plasma membranes, its fatty acid composition consists mostly of relatively long saturated chains (16:0, 18:0, and 24:0), but, in mammalian spermatozoa, SM and its related precursor ceramide (Cer) are made up of molecular species that contain very long-chain (24:0 to 34:0) polyunsaturated fatty acids N-linked to sphingosine (Poulos et al. 1986, 1987; Sandhoff 2010). These fatty acids, in proportions that vary among species, are elongated versions of common PUFA of the n-6 series (such as arachidonic or docosapentaenoic acids) or the n-3 series (such as eicosapentaenoic or docosahexaenoic acids). In some mammals, including rats, part of the very-long-chain polyunsaturated fatty acids (VLCPUFA) of sperm SM is 2-hydroxylated (Robinson et al. 1992; Furland et al. 2007).

Cer is a pivotal compound of high significance for metabolic signaling (Zheng et al. 2006; Hannun and Obeid 2011). It represents a converging point for both the synthetic and degradative pathways of SM and glycosphingolipids (Venkataraman and Futerman 2000; Tettamanti et al. 2003) and also regulates the content of diacylglycerol (Hampton and Morand 1989; Hannun et al. 2001), of some glycerophospholipids, and of other lipid messengers, such as the platelet activating factor. In such metabolic neworks, a sequence of transacetylase reaction activities are involved in the interconversion of 2:0 Cer with Cers of different chain lengths in cells and tissues (Abe et al. 1996; Merrill 2011). In cell membranes, molecular species of natural Cers are metabolically connected to SMs through the activity of different sphingomyelinases that remove the phosphocholine group irrespective of the N-acyl chain length of the substrate (Jungner et al. 1997; De Tullio et al. 2008). Also, some of these enzymes are endowed with phospholipase-A2-like activities that lead to the modification of glycerophospholipids hydrocarbon chain composition. Thus, the structural effect of a particular lipid in a cellular scenario can derive not only from its constituent moieties but also from the relationships among several enzymatic and metabolic networks that cross-communicate and become mutually modulated through biochemical and biophysical signals (Maggio et al. 2008).

A rather widespread idea of the functional importance of sphingolipids in cell membranes refers to the occurrence of ordered domains enriched in SM and Cer that are assumed to exist irrespective of the type of N-acyl chain in the sphingolipid. However, most studies dealing with such condensed and ordered domains, either in model or natural membranes, have employed compounds with acyl chains with 16 carbons and scarce attention has been devoted to understand the influence of variations of the N-acyl chain on the phase state and miscibility of the lipids. Even worse, the same concept is frequently applied when using sphingolipids derivatized with fluorescent probes to track the sphingolipid fate in cell biology studies, disregarding that such molecules have utterly different biophysical properties than the compound that is supposed to being tracked (Fanani and Maggio, unpublished). In addition, it is frequently disregarded that N-palmitoyl-Cer itself (the compound usually employed to extract conclusions about the properties of "Cer") exhibits complex temperature- and surface pressure-dependent phase transitions among various condensed and expanded states of different organization (Shah et al. 1995a; Fanani and Maggio 2010). Relatively small variations of the N-acyl chain length of Cers markedly affects their phase state, interfacial elasticity

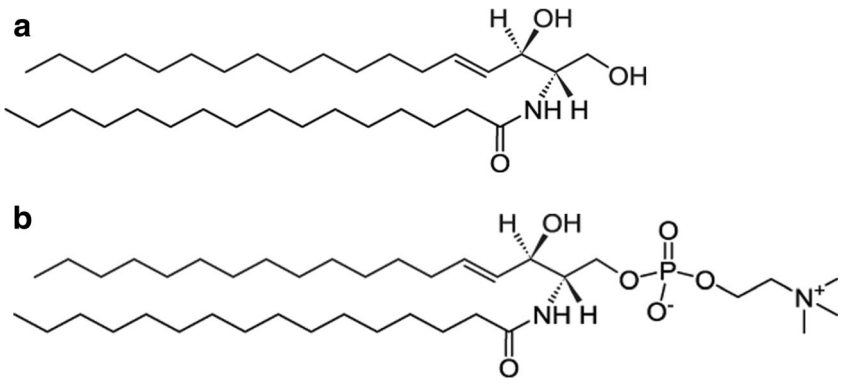

Scheme 1 Chemical structure of (**a**) 16:0 Cer and (**b**) 16:0 SM

domain thickness, surface topography, and electrostatics (Dupuy et al. 2011), and even condensed Cers can form liquid-like expanded states when interacting with Cers with particular hydrocarbon chain mismatch (Dupuy and Maggio 2012).

The chemical variety in the sphingolipid molecules is responsible for a large structural polymorphism. This is due to the intrinsic natural curvature imposed by the polar head group volume, in relation to that of the hydrocarbon moiety (Israelachvili 2011). For example, while gangliosides with a complex and charged head group self-assemble as micellar structures of different shapes and sizes (Maggio 1985; Cantu' et al. 2014), SMs and cerebrosides form stable bilayers (Koynova and Caffrey 1995). In the case of Cers, it has been reported that natural extracts of bovine brain- and N-palmitoyl-Cer can form lamellar stackings (Shah et al. 1995a), a feature also induced by other complex glycosphingolipids and some of their mixtures with PC (Maggio et al. 1988). However, when mixed with inverted phase-forming lipids such as phosphatidyl-ethanolamine, it was shown that Cers N-acylated with fatty acids equal or longer than 8 carbons decreased the temperature of lamellar L- to hexagonal II transition (Sot et al. 2005a), suggesting that this Cer stabilized the negative curvature of membranes. On the other hand, when mixed with dipalmitoyl PC, an increase of the main transition temperature and reduction of bilayer thickness due to chain interdigitation is induced by egg-Cer (Carrer and Maggio 1999).

The following sections, as well as the following article (Part II) that forms part of the present Special Issue, summarize further details related to the properties briefly introduced above.

Ceramides

16:0 Ceramide

A considerable amount of information has been published on the effects of 16:0 Cer in binary mixtures (Holopainen et al. 2000, 2001; Goñi and Alonso 2006, 2009; Busto et al. 2009; Karttunen et al. 2009; López-Montero et al. 2010), but comparatively little work has dealt with the physical properties of pure 16:0 Cer itself (Shah et al. 1995a; Chen et al. 2000), possibly because technical difficulties have been reported for reaching workable homogeneous samples at proportions of 16:0 Cer above 30 mol% (Holopainen et al. 2000; Busto et al. 2009), a situation also found for bovine brain Cer (Carrer and Maggio 1999). A complex thermotropic behavior was observed for the fully hydrated 16:0 Cer (Shah et al. 1995a). A metastable bilayer gel phase exists at low temperatures, with increasing temperature an exothermic transition occurs at 64 °C to form a stable bilayer probably chain-tilted with respect to the bilayer normal. Further increase in temperature leads to a disordered (likely HII-type) chain-melted phase (Tm 90 °C). These results were further supported by infrared studies (Chen et al. 2000). In monolayers, pure 16:0 Cer films exhibit an isothermal surface pressure-induced condensed–condensed phase transition at room temperature (Busto et al. 2009). Such transition occurs about 40 °C below the transition observed for bulk aqueous dispersions of 16:0 Cer (Shah et al. 1995a; Chen et al. 2000).

At room temperature, surface pressure–mean molecular area isotherms of pure 16:0 Cer apparently exhibit a transition-free condensed behavior previously reported (Maggio et al. 1978; Holopainen et al. 2001; Busto et al. 2009). However, more detailed studies showed that a diffuse, probably second-or higher-order, phase transition between two condensed phases that usually goes unnoticed can be detected as an inflection in the isotherm curve and compressibility modulus (Cs^{-1}) analysis (Fig. 1, black arrows). At temperatures 22–27 °C, the phases at low and high surface pressures showed Cs^{-1} values between 300 and 500 $mN.m^{-1}$ and 600 and 800 $mN.m^{-1}$, respectively. According to these values, such phases can be characterized as liquid condensed (LC) and solid (S), respectively (Davies and Rideal 1963). At 45 °C and above, a first-order liquid-expanded (LE)–LC phase transition is observed (Fig. 1, gray arrows) involving a large change in molecular area (77% increase at 10 $mN.m^{-1}$; see also Fig. 5). This phase shows Cs^{-1} values of ≈60 $mN.m^{-1}$, corresponding to a LE character (Davies and Rideal 1963; Smaby et al. 1996). The presence of a LE phase of Cers was previously reported only for N-stearoyl Cer at 5.7 $mN.m^{-1}$ at 52 °C (Fidelio et al. 1986). This is not very different from what is exhibited by 16:0 Cer (at 11 $mN.m^{-1}$ at 49 °C, see Fig. 1). A structural study in bulk dispersion of 16:0 Cer (Shah et al. 1995a) also described three phases: two lamellar bilayer gel phases and a chain-disordered phase at high temperature.

At relatively low temperatures, 16:0 Cer monolayers show a considerable hysteresis that reflects the irreversible storage of cohesion work that is reduced with increasing temperature. 16:0 Cer shows a less condensed behavior during the first compression and becomes more condensed during a second compression after expansion. This phenomenon implies that, once 16:0 Cer molecules are forced to closely pack and acquire the more condensed state, the intermolecular arrangement formed at high pressures is quite resilient under expansion (or, at least, its relaxation kinetics is much slower than the film expansion process). As reasonably expected, the increase of molecular thermal energy caused by increasing temperature leads to more favorable (or faster) reversibility.

Fig. 2 represents a two-dimensional phase diagram of 16:0 Cer monolayers. It shows the presence of two condensed phases and a LE phase. To further characterize the topography of the three phases observed in the isotherm and isobar studies, measurements of monolayer optical thickness were performed by BAM. Formation of three phases was found,

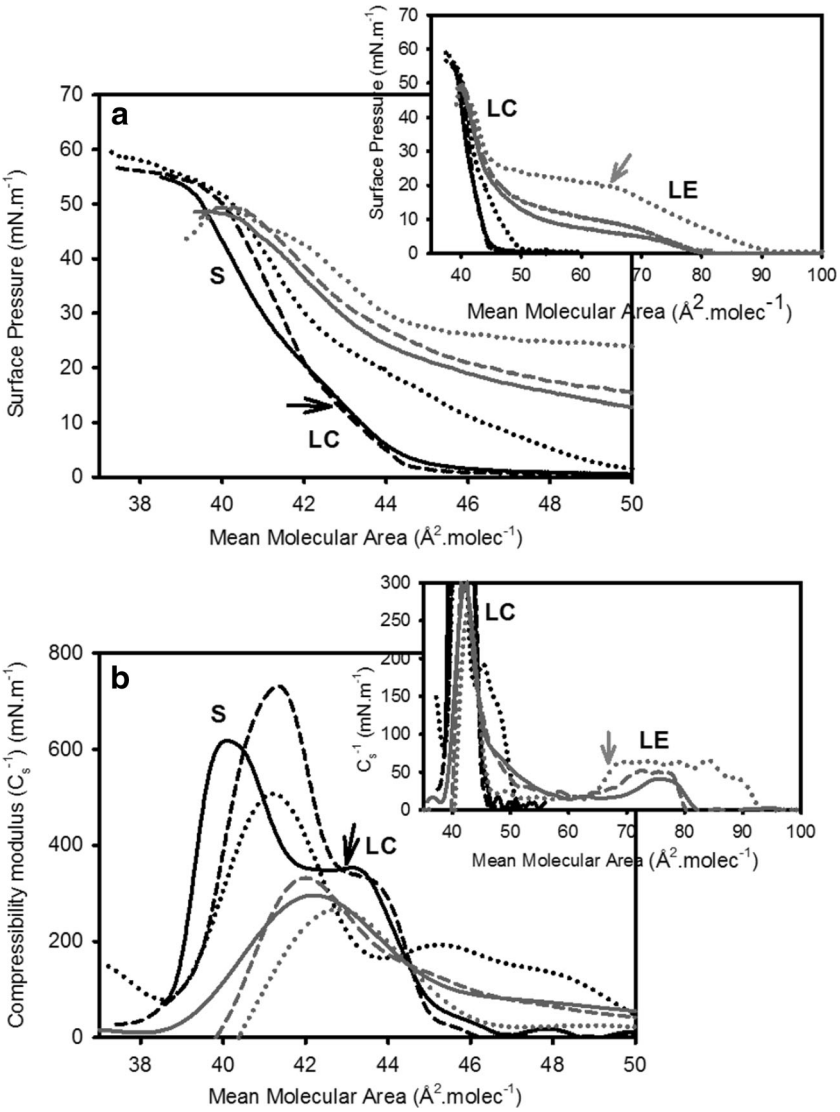

Fig. 1 First compression Isotherms of 16:0 Cer monolayers at different temperatures. Surface pressure (**a**) - and compressibility modulus (C_s^{-1}) (**b**): mean molecular area curves are shown for 16:0 Cer at 23 °C (*black full line*), 34 °C (*black dashed line*), 39 °C (*black dotted line*), 45 °C (*gray full line*), 49 °C (*gray dashed line*) and 62 °C (*gray dotted line*). Insets show an extended mean molecular area axis. *LE*, *LC* and *S* stand for liquid-expanded, liquid-condensed and solid phase state, respectively. Black arrows show the LC–S phase transition. *Gray arrows* show the beginning of the LE–LC phase transition. The *curves* show a single representative experiment from a set of triplicates. Reprinted from Fanani and Maggio (2010), with permission from Elsevier

depending on the surface pressure and temperature: a solid (1.80 nm thick), a LC (1.73 nm thick, likely tilted) and a LE (1.54 nm thick) phase over the temperature range 5–62 °C. A large hysteretic behavior is observed for the S phase monolayer that can be due to its high resistance to domain boundary deformation. A second- (or higher-) order S → LC phase transition is observed at about room temperature while a first-order LE → LC transition occurs in a range of temperature encompassing the physiological range (observed from 30 °C at low surface pressure). This phase behavior clearly emphasizes that Cer is not always rigid but able to exhibit a rich polymorphism depending on the relative strength of molecular interaction compared to the molecular thermal energy determined by temperature. This is a quite important concept because it means that a phase change in Cer can occur even isothermally whenever the molecular interactions fall below the thermal energy.

Short-chain ceramides

Long-chain Cers are highly hydrophobic, essentially insoluble and non-dispersible in aqueous solution. Thus, short-chain Cers are commonly used in cell culture studies even if their biological action and most of their physical properties are entirely different from those of their long-chain analogues (Ghidoni et al. 1999; Sot et al. 2005b). In lipid monolayers at the air–water interface, the molecular packing, dipole potential, in plane elasticity, physical state, interfacial thickness, and morphology of the condensed domains formed by Cer is highly dependent on the length of the N-acyl chain. These represent further levels of modulation of the information transduction capacity of Cer through supramolecular amplification of molecular changes determined by metabolism.

The variation of the surface pressure and perpendicular dipole moment as a function of the mean molecular area is quite

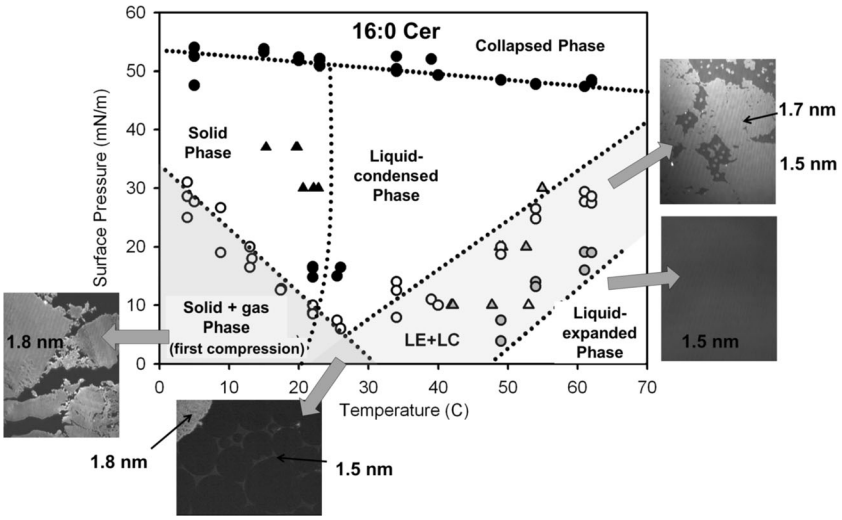

Fig. 2 Phase diagram for 16:0 Cer monolayers. Surface pressure vs. temperature phase diagram of 16:0 Cer from isotherms (*circles*) and isobars (*triangles*) data. A solid, a liquid-condensed (*LC*) and a liquid expanded (*LE*) phase are identified in the temperature and pressure range explored. Additionally, the collapse point of each isotherm provides information of the transition to the collapsed phase. *Black symbols* correspond to second-order transitions, *gray and white symbols* correspond to the beginning and the end of first-order transitions, respectively. The *gray shadowed areas* indicate phase coexistence regions: the *bottom left triangle* indicates gas–solid coexistence only for the first compression of the monolayer; the *small triangle in the bottom center* is a three-phase (LC/LE/gas) coexistence region and the *shadowed area* on the *right* corresponds to a LC–LE coexistence region. Image size 372 × 466 μm. The data correspond to the whole set of experiments where each point corresponds to a single experiment. The images are representative experiments. Modified from Fanani and Maggio (2010)

different for N-acyl Cers of different length. As expected, Cers with N-acyl chain length less than 14 carbon atoms form interfaces with a more LE character. Also, surface-pressure-induced two-dimensional phase transitions occur in these molecules (Fig. 3). This is in general agreement with the progressively lower temperatures of the stable main phase transition of Cers aqueous dispersions with the shortening of N-acyl chains (Westerlund et al. 2010). The inset in Fig. 3 shows that, after the Cer films reached a coherent state, the variations of the magnitude of the resultant perpendicular dipole moment also reflects the phase state of the films with the dipolar rearrangements occurring in coincidence with the LE–LC transitions.

Changes of the length of the saturated fatty acid N-linked to sphingosine produced conspicuous changes of the Cer interfacial behavior. 16:0 Cer exhibits S–LC and LE–LC transitions induced by variations of surface pressure over the physiological temperature range (Fanani and Maggio 2010). Shorter fatty acid chain lengths loosen intermolecular interactions and LE phases occur in 12:0 Cer and 10:0 Cer at 21 °C. The higher surface pressure necessary for taking 10:0-Cer to a condensed state, compared to that required by 12:0 Cer (22 vs. 2 $mN.m^{-1}$, respectively), points out the dramatic importance of the chain–chain interactions for acquiring the condensed state in Cers. On the other hand, the four Cers studied essentially showed the same limiting cross-sectional area at collapse (between 38 and 40 $Å^2$. $molecule^{-1}$) which can be accounted for by close packing of both the fatty acyl and sphingosine chains while the small polar headgroup of Cer does not contribute to the cross-sectional area of the lipid in the condensed state, as reported earlier (Lofgren and Pascher 1977; Maggio et al. 1978). The difference in length (mismatch) of the N-linked palmitoyl chain of 16:0 Cer and the 18C of the sphingosine is negligible. However, when the chain asymmetry increases, mismatch compensations can occur and one such effect in lipid bilayers is the establishment of chain interdigitation (Huang and McIntosh 1997) that has been demonstrated in SM (Boggs and Koshy 1994) and asymmetric Cers (Carrer et al. 2003, 2006).

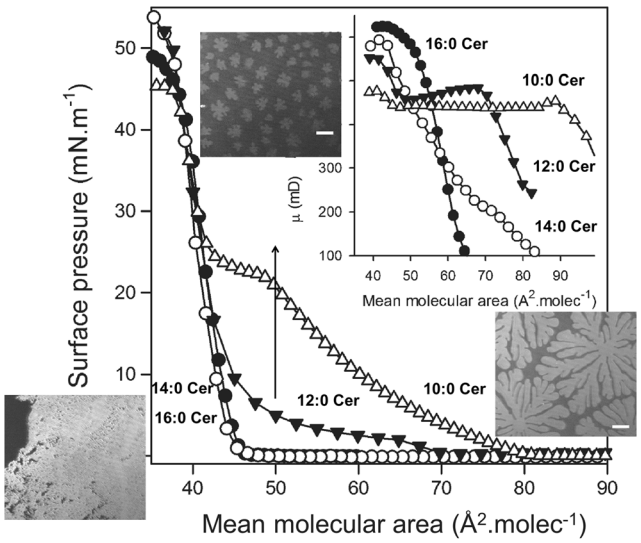

Fig. 3 Surface pressure–molecular area isotherms and dipole potential (*inset*) of Langmuir monolayer of ceramides. (●) 16:0 Cer, (O) 14:0 Cer, (▼) 12:0 Cer, and (Δ) 10:0 Cer. Measurements were performed at 21 °C. Extracted from Dupuy et al. (2011)

On the other hand, interdigitation is not possible in monolayers because there is no hydrocarbon layer above the chains. In the condensed state, both chains are pointing out into the air side of the interface. In such a case, the film thickness should correspond to that of the longer hydrocarbon moiety of sphingosine and approximately the same in all the Cers studied. However, film thickness of the condensed phase increased in proportion to the length of the N-linked fatty acid chain length (Fig. 4a). The resultant perpendicular dipole moment, calculated from surface potential measurements, varies as the film is taken to different phase states determined by the surface pressure. The maximum values corresponded to the more condensed state of each Cer, and their magnitude also correlates linearly with film thickness (Fig. 4b). 16:0 Cer and 10:0 Cer have the largest and the smallest dipole moments of the series studied, respectively, indicating that the N-acyl chains contribute to the molecular dipole of Cers in proportion to their length.

A possible explanation of the reduced thickness of 10:0 Cer and 12:0 Cer is that a portion of the sphingosine chain (which is the same in all the Cers studied) may bend over the N-acyl chain (Fig. 4c). The values of the resultant perpendicular dipole moment are also in keeping with a bending of the exceeding hydrocarbon segment of the sphingosine moiety over the length of the shorter N-fatty acid chain. These electrostatic data, together with the independent measurements of the limiting molecular areas, of the interfacial thickness, and the geometrical analysis discussed above are in keeping with the possibility that in monolayers of asymmetric short chain Cers at the closest packing, the sphingosine chain could bend over the N-linked fatty acyl chain thus reducing hydrophobic mismatch while maximizing hydrocarbon interactions. In a lipid bilayer containing asymmetric Cers, chain interdigitation can occur, instead of bending, which is compatible with the observed reduction of bilayer thickness and chain length-dependence of paramagnetic probe mobility (Carrer et al. 2003, 2006).

Long- and unsaturated chain ceramides

Different to 16:0 Cer and 18:0 Cer nonhydroxyl Cers that show a condensed character, the introduction of a double bond at C9 in the amide-bound fatty acid of Cer, as in 9Δ18:1 Cer, leads to expanded monolayers (Fig. 5). However, when the double bond occurs at the C15 of the N-linked acyl hydrocarbon chain, as in 15Δ24:1 Cer, the molecules can still pack into an LC phase at room temperature and exhibit an LC→S transition quite similar to that shown by the saturated 16:0 Cer (Lofgren and Pascher 1977; Peñalva et al. 2014a).

A combined elongation and polyunsaturation of the N-acyl chain of Cers results in the occurrence of very-long-chain, polyunsaturated fatty acids (VLCPUFA) Cers, such as the purified from rat testes (Peñalva et al. 2014a). VLCPUFA-containing Cers species show both an LE and an LC phase at room temperature (Fig. 5). Counting from the amide-bound carbon, the first of the series of 4 or 5 methylene-interrupted cis double bonds of the Cer species of VLCPUFA Cers are located at C12, C13 and C14 in the 30:5, 28:4 and 32:5 acyl chains, respectively, at an intermediate location between the two above-mentioned monounsaturated Cers. Then, a minimum saturated portion of C12 appears to be sufficient to favors the occurrences of a LC phase, facilitating van der Waals interactions among acyl chains. Ordinary Cers in their LC or S state typically occupy an area of ~40–42 $Å^2$.$molecule^{-1}$ which is roughly the lower limiting cross-sectional area for lipids with two-tailed, fully extended saturated acyl chains. However, nonhydroxy VLCPUFA Cers remarkably show up to 3.4 - fold larger area than 18:1 Cer in its LE state (Fig. 5). The former phase appears as a consequence of the hydrocarbon chain disordering thus reducing the tightness of their packing by their several double bonds but not inducing a thicker film than other Cer monolayers (Peñalva et al. 2014a).

In many tissues, a considerable number of the sphingolipid species contain a 2-hydroxyl group at the

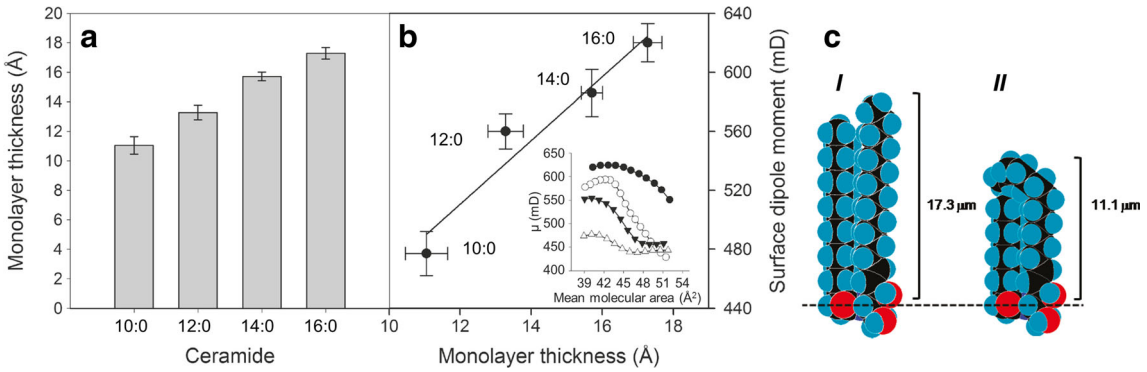

Fig. 4 Film thickness of the ceramides in the condensed phase measured at 37 $mN.m^{-1}$ (**a**). Correlation between film thickness and maximum dipole moment of the condensed phase of ceramides (**b**). *Inset* resultant perpendicular dipole of the condensed phase of 10:0 Cer (Δ), 12:0 Cer (▼), 14:0 Cer (O), and 16:0 Cer (●). Results are the average of three independent experiments. **c** Molecular models generated with Alchemy III software (Tripos Ass.) of 16:0 Cer (*I*) and the proposed arrangement of 10:0 Cer (*II*) with the sphingosine chain bending over the N-acyl chain. The *scales* indicate monolayer thickness measured by BAM, and the *dashed line* shows the probable location of the interface. Modified from Dupuy et al. (2011)

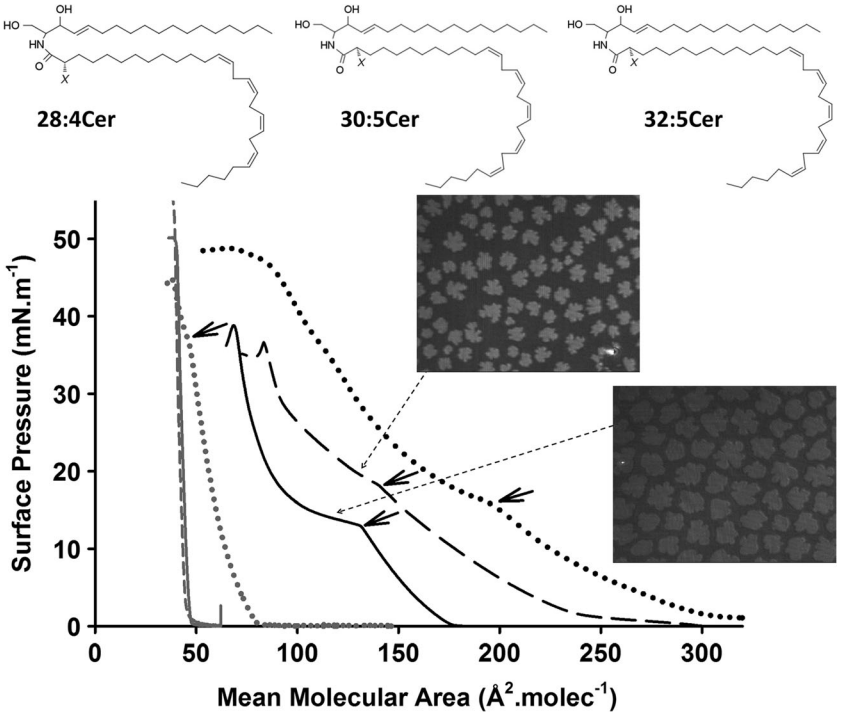

Fig. 5 Schematic structures of the ceramides containing nonhydroxy and 2-hydroxy very-long-chain polyunsaturated fatty acids (VLCPUFA) purified from rat testes. *X* represents the presence of –H or –OH, respectively, in the second carbon atom of the amide-bound fatty acid. The plot shows compression isotherms of the nonhydroxilated Cer serie: 16:0 Cer (*gray full line*) and 18:1 Cer (*gray dotted line*), 24:1 Cer (*gray dashed line*), 28:4 Cer (*black full lines*), 30:5 Cer (*black dashed lines*) and 32:5 Cer (*black dotted lines*). The *short arrows* indicate the beginning of the LE to LC phase transition. Micrographs (size 200 × 250 μm) correspond to Brewster angle microscopy images of monolayers of VLCPUFA-containing ceramides through the LE–LC transition region. Adapted from Peñalva et al. (2014a)

second carbon atom of their fatty acyl chain. This biochemical modification also occurs in the VLCPUFA of rodent testis sphingolipids including SMs and Cers (Zanetti et al. 2010). The 2-hydroxy VLCPUFA Cers show similar surface behavior to their nonhydroxylated relatives but showing smaller molecular areas; this is evidencing an important contribution of the 2-hydroxyl group placed near the air-water interface in their capacity for close molecular packing (Peñalva et al. 2014a). The change of phase transition pressure with temperature provides thermodynamic data that allow an estimation of the melting temperature of the sphingolipids should they be organized in bilayers (Maggio 1994). This extrapolation suggests that both nonhydroxy and 2-hydroxy 28:4 Cer underwent melting at 45–46 °C. On the other hand, a large difference was calculated for the nonhydroxy versus the 2-hydroxy 30:5 Cer, giving melting temperatures of ~36 and ~53 °C, respectively (Peñalva et al. 2014a). Those values indicate that the VLCPUFA Cers studied might organize in a gel state at the physiological temperature but close to their phase transition points. Subtle changes of temperature, and/or a drop in surface pressure due to thermal fluctuations, could then induce an LC–LE phase transition of these molecules, involving a large molecular lateral expansion. Since the Cer polar headgroup is very small, such lateral expansion would concomitantly translate into changes of the geometry of the Cer molecules and the overall membrane curvature.

It is worth noting that the Cs^{-1} values for the LC phases formed by all Cers species containing VLCPUFA were lower than those obtained for shorter Cers. Considering the usual classification of lipid monolayers state according to the value of Cs^{-1} (Davies and Rideal 1963), the VLCPUFA Cer films could be expected to be in a LE rather than in a LC state. In order to unravel this discrepancy, the Brownian motion of micrometer-sized latex beads placed onto 2-hydroxyl 28:4 Cer films were analyzed in comparison with shorter Cer films (Peñalva et al. 2014b). 18:1Cer films in the LE state allow a high lateral diffusion of latex beads whilst, similar to 16:0 Cer LC films, 2-hydroxyl 28:4 Cer monolayers allow a very restricted lateral diffusion. Therefore, the diffusion parameters, rather than the compressibility properties, describe pure 2-hydroxyl 28:4 Cer films as being in a soft-condensed phase state at high molecular surface density (Peñalva et al. 2014b). This unusual highly compressible LC phase appears compatible with a high conformational freedom of the bended and partially hydrated VLCPUFA moieties but having the characteristically low diffusional properties of a LC phase. This resembles the rheological properties described for polymer monolayers in a semi-dilute regime and good solvent

conditions in which an interpenetrated network of the long-chained structures leads to chain entanglement reptating motion. Such atypical rheological properties have only been described for VLCPUFA Cer films among all naturally occurring lipid membranes studied so far.

Topological implications

Natural extracts of bovine brain and 16:0 Cer form lamellar stackings (Shah et al. 1995a), a feature also induced by other complex glycosphingolipids and some of their mixtures with PC (Maggio et al. 1988). However, when mixed with inverted phase-forming lipids such as phosphatidylethanolamine, Cers N-acylated with fatty acids equal to or longer than 8 carbons decreased the temperature of lamellar Lα to hexagonal II transition (Sot et al. 2005a), suggesting that this Cer stabilizes the negative curvature of membranes. On the other hand, when mixed with dipalmitoyl PC, an increase of the main transition temperature and a reduction of bilayer thickness due to chain interdigitation is induced by egg-Cer (Carrer and Maggio 1999). Natural Cers (mostly constituted by 16:0 and 18:0 N-acyl chains) display a high transition temperature (Fidelio et al. 1986; Shah et al. 1995b; Westerlund et al. 2010), owing to tight molecular packing, high van der Waals interactions and subsequent hydrogen bonding (López-Montero et al. 2010). In bilayer and monolayer model systems, such Cers form highly ordered, solid phases (López-Montero et al. 2010; Dupuy et al. 2011; Castro et al. 2014) and, when mixed with either glycerophospholipids or sphingolipids, induce phase segregation of condensed domains and complex thermograms (Busto et al. 2009; Westerlund et al. 2010; Pinto et al. 2011; Dupuy and Maggio 2014).

In Langmuir monolayers, 10:0 Cer at 24 °C show an expanded to condensed transition (Dupuy et al. 2011) at about 25 mN m^{-1}, a surface pressure higher than the transition pressure of 16:0 SM (16:0 SM) (Smaby et al. 1996; Ramstedt and Slotte 1999; Busto et al. 2009; Dupuy and Maggio 2014) which is about 12 mN.m^{-1}. This implies a less solid character of the short-chain Cer compared to the symmetric SM. However, this trend is not followed by the behavior of these lipids in bulk. The main transition temperature of 10:0 Cer dispersed in bulk is higher than that of 16:0 SM (Ramstedt and Slotte 1999) (75 vs. 41 °C, respectively) indicating a less solid character of the SM. This indicates that the arrangement of the molecules in the planar geometry in monolayers at the air–water interface is not preserved in 10:0 Cer when dispersed in bulk, at variance with the bilayer-forming 16:0 SM.

Using small-angle X-ray scattering and polarized light microscopy, the fully hydrated 10:0 Cer dispersions, at temperatures below the main transition, are arranged in a tridimensional structure corresponding to an inverted hexagonal phase (Dupuy et al. 2017). Infrared spectroscopy and wide angle X-ray diffraction indicate that the acyl chains of Cers exhibit a relatively high order in the hexagonal phase (Fig. 6). As far as we know, this is the first report of a lipid hexagonal phase having highly ordered acyl chains. Molecular asymmetry due to the different length of the sphingosine and the N-acyl chains of 10:0 Cer may explain the formation of this novel phase in which the topological stress arising from the "void" volume between lipid tubules arranged in hexagonal lattice is reduced by the chain asymmetry; the portion of the sphingopid hydrocarbon chain exceeding the length of the N-acyl chain fills the void volume in the hexagonal arrangement. Topologically, this would resemble the chain interdigitation known to occur in bilayers containing asymmetric Cers with 10:0 or 8:0 N-acyl chains (Carrer et al. 2003, 2006).

Sphingomyelins

Like PC, SM has phosphocholine as its zwitterionic polar headgroup. SM and PC both have two long hydrocarbon chains configured in rather similar ways. In PC, both hydrocarbon chains are ester-linked to a glycerol backbone, the *sn*-1 chain is usually saturated and the *sn*-2 chain usually contains one or more *cis* double bonds. By contrast, in SM the sphingoid base serves a dual role as both interfacial backbone and nonpolar hydrocarbon chain. The only true acyl chain is amide-linked. The structural features that may enable SM to provide a specialized membrane environment include (1) an abundance of long, saturated acyl chains that sometimes provide intramolecular chain-length asymmetry, and (2) interfacial functional groups that can donate and accept hydrogen bonds with neighboring lipids (Barenholz and Thompson 1980; Boggs 1987). SM bilayers predominantly occur with intermolecular SM–SM hydrogen bonds in the gel state but intramolecular or SM–water hydrogen bonds are more frequent in the liquid disordered phase (Niemelä et al. 2004). This implies a high potential for SM to interact (also through hydrogen bonding) with soluble amphiphilic proteins when organized in the disordered state (Pedrera et al. 2014), since it would avoid extensive breaking of stronger SM–SM hydrogen bonding that are established in the gel state.

Only relatively recently has the importance of acyl chain length and saturation begun to be recognized as an important structural feature in SM's interactions with other lipids (e.g., Silvius 1992; Smaby et al. 1994, 1996; Silvius et al. 1996; Ahmed et al. 1997). Despite the fact that saturated chains of differing lengths dominate the acyl composition of most naturally occurring SMs, the effect of changing acyl chain length on the physical behavior of SM remains poorly understood (Snyder and Freire 1980; Maulik et al. 1986; Sripada et al. 1987; Bar

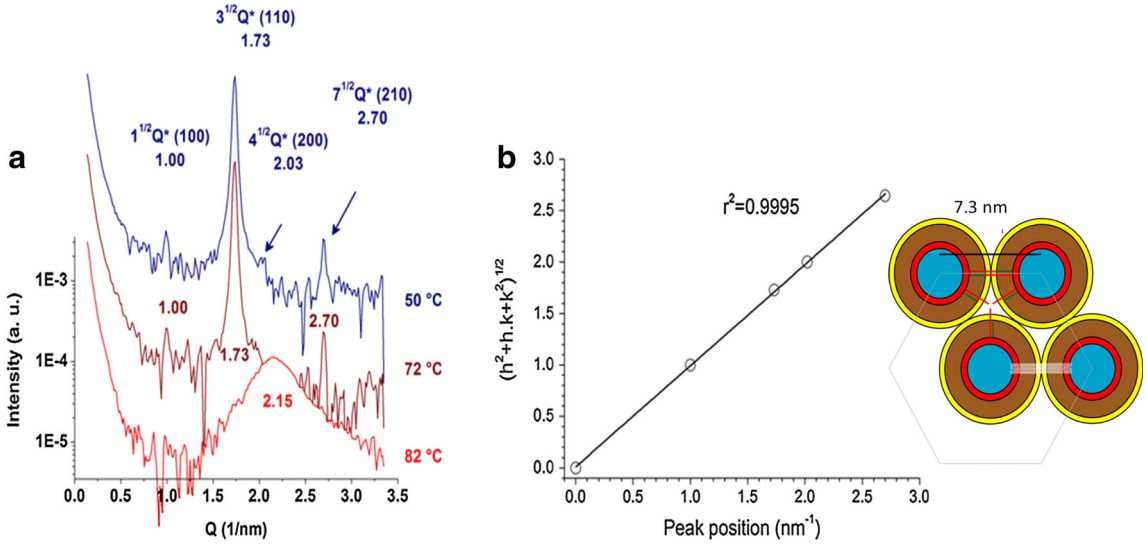

Fig. 6 Structural analysis of 10:0 ceramide aqueous suspension. **a** SAXS patterns of 10:0 Cer at the indicated temperatures in the hexagonal phase (*blue* and *brown*) and disordered phase (red). Synchrotron radiation was used and spectra were acquired after 10 min of thermal stabilization. Measurements were carried out in triplicate with fresh samples. **b** Correlation of the position of the SAXS peaks with Miller indexes of a hexagonal crystal array. The scheme show a simplified model of the HII tubular micelles represented in cross-section. The main slabs are shown in color: *blue* for water, *red ring* for polar headgroup, *brown ring* for the non-interdigitated acyl chain region, *yellow ring* for the asymmetric (interdigitated) region of the acyl chains, *green stick* (acyl chain of 10 carbonyls), *red stick* for the acyl part of sphingosine and *white* is the packing frustration region. The remarkable feature of this cartoon is that the sphingosine methyl end practically fit close to the center of the space between the cylinders, relieving packing frustration. Adapted from Dupuy et al. (2017)

et al. 1997; Ramstedt and Slotte 1999; Peñalva et al. 2014b). Careful systematic studies on the dependence of the surface behavior of SMs with different N-linked acyl chains (12:0, 14:0, 16:0, 18:0, 24:0, 26:0) have been reported (Li et al. 2000), and readers are referred to this excellent work. Briefly, SM containing lauroyl (C12:0) acyl chains displayed only LE behavior. Increasing the length of the saturated acyl chain (e.g., 14:0, 16:0, or 18:0) resulted in LE to LC two-dimensional phase transitions at temperatures in the 10–30 °C range. Similar behavior was observed for SMs with lignoceroyl (24:0) or cerotoyl (26:0) acyl chains, but isotherms showed only condensed behavior at 10 and 15 °C.

Insights into the interactions occurring within the different SM phases, and accompanying changes in SM phase state were provided by analyzing the in-plane elasticity using the compressibility moduli. At similar surface pressures, LE phases of SM were less compressible than those of PCs with

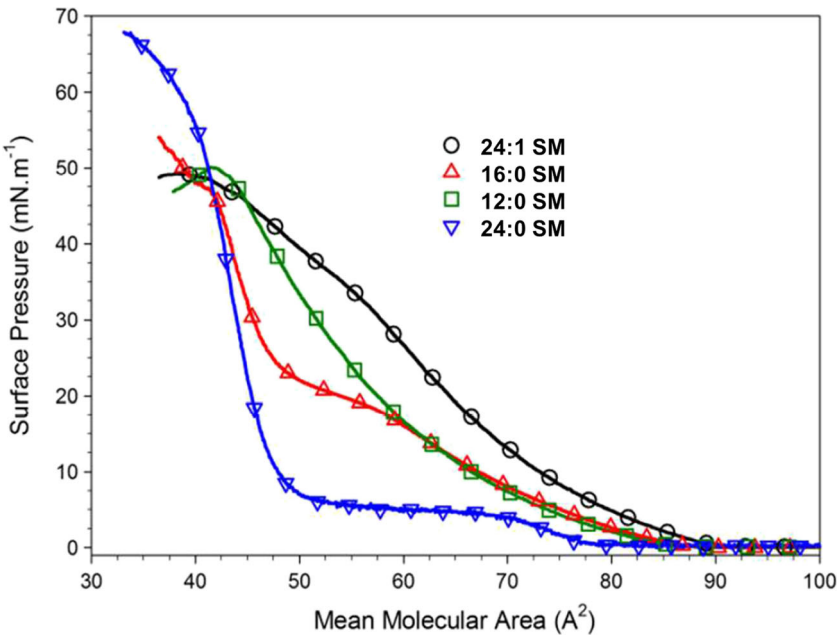

Fig. 7 Compression isotherms at 24 °C of sphingomyelin monolayers N-acylated with different fatty acids. Reprinted with permission from Dupuy and Maggio (2014), Copyright 2014 American Chemical Society

similar chain structures. The area per molecule and compressibility of SM condensed phases depend upon the length of the saturated acyl chain (Fig. 7) and upon the spreading temperature. Spreading of SMs with very long saturated acyl chains at temperatures 30–35 °C below the bulk T_m resulted in condensed films with lower in-plane compressibility, but consistently larger cross-sectional molecular areas than the condensed phases achieved by spreading at temperatures only 10–20 °C below *T*m. Fig. 7 shows results reproducing some of the findings summarized above.

VLCPUFA-containing SMs form a quite disordered LE phase when organized in a monolayer, showing large areas per molecule and low film thickness (Peñalva et al. 2014b). The nonhydroxy 32:5 SM appears as the most expanded one with low Cs^{-1} values a molecular area 80% larger than the 18:1 SM also in the LE phase state. This implies rather weaker intermolecular interactions, and in general tends to be more fluid compared to those occurring between SMs with relatively shorter and straight-chain saturated fatty acids. Similar to VLCPUFA-containing Cers, the 2-hydroxy SMs show smaller molecular areas. Then, as a general behavior, the presence of the 2-hydroxyl group in the fatty acid of both SMs and Cers favors stronger intermolecular interactions leading to more compact surface packing. Evidences of a similar effect was observed also in bilayers, where 2-hydroxy VLCPUFA SMs increases the degree of order to a larger extent than their chain-matched nonhydroxy VLCPUFA SMs (Peñalva et al. 2013).

Upon cooling, only the longest nonhydroxy 32:5 SM and 2-hydroxy 32:5 SM shows an LE → LC phase transition in monolayers and also a transition upon heating, close to room temperature, in bilayers (Peñalva et al. 2013, 2014b). Finally, VLCPUFA-containing SMs show a large conformational freedom that opposes lateral compression. However, the loss of entropy of the VLCPUFA upon compression appears to be counteracted by a released of the hydration shell of the phosphocholine groups (Peñalva et al. 2014b), an effect supported by dynamic simulation studies that evidence a more structured hydration water at the surface of SM membranes in comparison with PCs (Niemelä et al. 2004).

In summary, variations of the N-acyl chain length in ceramides and sphingomyelins markedly affect their phase state, electrostatics and interfacial elasticity, which in turn result in a rich variety of patterns at the surface topography level. Furthermore, these properties condition the tridimensional structure of the membrane at an even higher structural level. Thus, the usually conceived concept of "condensed" sphingolipids should be revised in the light of the evidences shown here. Additionally, the miscibility properties of ceramides and spingomyelins in binary mixtures of different composition, and with other more complex sphingolipids, are also strongly regulated by the variations in their N-acyl chains. This issue will be analyzed and discussed in the part II of this revision work.

Acknowledgments This work was supported by the Consejo Nacional de Investigaciones Científicas y Técnicas (CONICET), Agencia Nacional de Promoción Científica y Tecnológica (ANPCyT, FONCyT PICT 2014-1627), and the Secretary of Science and Technology of Universidad Nacional de Córdoba (SECyT-UNC), Argentina.

Compliance with ethical standards

Conflicts of interest María Laura Fanani declares that she has no conflicts of interest. Bruno Maggio declares that he has no conflicts of interest.

Ethical approval This article does not contain any studies with human participants or animals performed by any of the authors.

References

Abe A, Shayman JA, Radin NS (1996) A novel enzyme that catalyzes the Esterification of N-Acetylsphingosine. J Biol Chem 271:14383–14389

Ahmed SN, Brown D a, London E (1997) On the origin of sphingolipid/cholesterol-rich detergent-insoluble cell membranes: physiological concentrations of cholesterol and sphingolipid induce formation of a detergent-insoluble, liquid-ordered lipid phase in model membranes. Biochemistry 36:10944–10953. doi:10.1021/bi971167g

Bar LK, Barenholz Y, Thompson TE (1997) Effects of sphingomyelin composition on the phase structure of phosphatidylcholine-sphingomyelin bilayers. Biochemistry 36:2507–2516

Barenholz Y, Thompson TE (1980) Sphingomyelins in bilayers and biologicas membranes. Biochim Biophys Acta 604:129–158

Boggs JM (1987) Lipid intermolecular hydrogen bonding: influence on structural organization and membrane function. Biochim Biophys Acta 906:353–404. doi:10.1016/0304-4157(87)90017-7

Boggs JM, Koshy KM (1994) Do the long fatty acid chains of sphingolipids interdigitate across the centre of a bilayer of shorter chain symetric phospholipids? Biochim Biophys Acta - Biomembr 1189:233–241

Busto JV, Fanani ML, De Tullio L et al (2009) Coexistence of immiscible mixtures of palmitoylsphingomyelin and palmitoylceramide in monolayers and bilayers. Biophys J 97:2717–2726. doi:10.1016/j.bpj.2009.08.040

Cantu' L, Del Favero E, Brocca P, Corti M (2014) Multilevel structuring of ganglioside-containing aggregates: from simple micelles to complex biomimetic membranes. Adv Colloid Interf Sci 205:177–186. doi:10.1016/j.cis.2013.10.016

Carrer DC, Härtel S, Mónaco HL, Maggio B (2003) Ceramide modulates the lipid membrane organization at molecular and supramolecular levels. Chem Phys Lipids 122:147–152. doi:10.1016/S0009-3084(02)00185-8

Carrer DC, Maggio B (1999) Phase behavior and molecular interactions in mixtures of ceramide with dipalmitoylphosphatidylcholine. J Lipid Res 40:1978–1989

Carrer DC, Schreier S, Patrito M, Maggio B (2006) Effects of a short-chain ceramide on bilayer domain formation, thickness, and chain mobililty: DMPC and asymmetric ceramide mixtures. Biophys J 90:2394–2403. doi:10.1529/biophysj.105.074252

Castro BM, Prieto M, Silva LC (2014) Ceramide: a simple sphingolipid with unique biophysical properties. Prog Lipid Res 54:53–67. doi:10.1016/j.plipres.2014.01.004

Chen HC, Mendelsohn R, Rerek ME, Moore DJ (2000) Fourier transform infrared spectroscopy and differential scanning calorimetry studies of fatty acid homogeneous ceramide 2. Biochim Biophys Acta Biomembr 1468:293–303. doi:10.1016/S0005-2736(00)00271-6

Davies JT, Rideal EK (1963) Interfacial Fenomena

De Tullio L, Maggio B, Fanani ML (2008) Sphingomyelinase acts by an area-activated mechanism on the liquid-expanded phase of sphingomyelin monolayers. J Lipid Res 49:2347–2355. doi:10.1194/jlr.M800127-JLR200

Dupuy F, Fanani ML, Maggio B (2011) Ceramide N-acyl chain length: a determinant of bidimensional transitions, condensed domain morphology, and interfacial thickness. Langmuir 27:3783–3791

Dupuy F, Maggio B (2012) The hydrophobic mismatch determines the miscibility of ceramides in lipid monolayers. Chem Phys Lipids 165:615–629. doi:10.1016/j.chemphyslip.2012.06.008

Dupuy FG, Fernández Bordín SP, Maggio B, Oliveira RG (2017) Hexagonal phase with ordered acyl chains formed by a short chain asymmetric ceramide. Colloids Surf B 149:89–96. doi:10.1016/j.colsurfb.2016.10.009

Dupuy FG, Maggio B (2014) N-acyl chain in ceramide and sphingomyelin determines their mixing behavior, phase state, and surface topography in langmuir films. J Phys Chem B 118:7475–7487. doi:10.1021/jp501686q

Fanani ML, Maggio B (2010) Phase state and surface topography of palmitoyl-ceramide monolayers. Chem Phys Lipids 163:594–600

Fidelio GD, Maggio B, Cumar F a (1986) Molecular parameters and physical state of neutral glycosphingolipids and gangliosides in monolayers at different temperatures. Biochim Biophys Acta 854:231–239. doi:10.1016/0005-2736(86)90115-X

Furland NE, Oresti GM, Antollini SS et al (2007) Very long-chain polyunsaturated fatty acids are the major acyl groups of sphingomyelins and ceramides in the head of mammalian spermatozoa. J Biol Chem 282:18151–18161. doi:10.1074/jbc.M700709200

Ghidoni R, Inserm U, Cellulaire B (1999) Use of sphingolipid analogs: benefits and risks. Biochim Biophys Acta 1439: 17–39

Goñi FM, Alonso A (2009) Effects of ceramide and other simple sphingolipids on membrane lateral structure. Biochim Biophys Acta Biomembr 1788:169–177. doi:10.1016/j.bbamem.2008.09.002

Goñi FM, Alonso A (2006) Biophysics of sphingolipids I. Membrane properties of sphingosine, ceramides and other simple sphingolipids. Biochim Biophys Acta Biomembr 1758:1902–1921. doi:10.1016/j.bbamem.2006.09.011

Hakomori SI (1990) Bifunctional role of glycosphingolipids: modulators for transmembrane signaling and mediators for cellular interactions. J Biol Chem 265:18713–18716

Hampton RY, Morand OH (1989) Sphingomyelin synthase and Pkc activation. Science 246(80):1050

Hannun Y a, Bell RM (1989) Functions of sphingolipids and sphingolipid breakdown products in cellular regulation. Science 243:500–507. doi:10.1126/science.2643164

Hannun Y a, Luberto C, Argraves KM (2001) Enzymes of sphingolipid metabolism: from modular to integrative signaling. Biochemistry 40:4893–4903. doi:10.1021/bi002836k

Hannun Y a, Obeid LM (2011) Many ceramides. J Biol Chem 286:27855–27862. doi:10.1074/jbc.R111.254359

Holopainen JM, Brockman HL, Brown RE, Kinnunen PK (2001) Interfacial interactions of ceramide with dimyristoylphosphatidylcholine: impact of the N-acyl chain. Biophys J 80:765–775. doi:10.1016/S0006-3495(01)76056-0

Holopainen JM, Lemmich J, Richter F et al (2000) Dimyristoylphosphatidylcholine/C16:0-ceramide binary liposomes studied by differential scanning calorimetry and wide- and small-angle x-ray scattering. Biophys J 78:2459–2469. doi:10.1016/S0006-3495(00)76790-7

Huang C, McIntosh TJ (1997) Probing the ethanol-induced chain interdigitations in gel-state bilayers of mixed-chain phosphatidylcholines. Biophys J 72:2702–2709. doi:10.1016/S0006-3495(97)78913-6

Israelachvili JN (2011) Soft and biological structures. In: Israelachvili JN (ed) Intermolecular and surface forces. Academic, San Diego, pp 535–576

Jungner M, Ohvo H, Slotte JP (1997) Interfacial regulation of bacterial sphingomyelinase activity. Biochim Biophys Acta - Lipids Lipid Metab 1344:230–240. doi:10.1016/S0005-2760(96)00147-6

Karttunen M, Haataja MP, Saily M et al (2009) Lipid domain morphologies in phosphatidylcholine-ceramide monolayers. Langmuir 25:4595–4600. doi:10.1021/la803377s

Koynova R, Caffrey M (1995) Phases and phase transitions of the sphingolipids. Biochim Biophys Acta 1255:213–236. doi:10.1016/S0304-4157(98)00006-9

Li XM, Smaby JM, Momsen MM et al (2000) Sphingomyelin interfacial behavior: the impact of changing acyl chain composition. Biophys J 78:1921–1931. doi:10.1016/S0006-3495(00)76740-3

Lofgren H, Pascher I (1977) Molecular arrangemets of sphingolipids. The monolayer behaviour of ceramides. Chem Phys Lipids 20:273–284

López-Montero I, Monroy F, Vélez M, Devaux PF (2010) Ceramide: from lateral segregation to mechanical stress. Biochim Biophys Acta Biomembr 1798:1348–1356. doi:10.1016/j.bbamem.2009.12.007

Maggio B (1994) The surface behavior of glycosphingolipids in biomembranes: a new frontier of molecular ecology. Prog Biophys Mol Biol 62:55–117. doi:10.1016/0079-6107(94)90006-X

Maggio B (1985) Geometric and thermodynamic restrictions for the self-assembly of glycosphingolipid-phospholipid system.Pdf. Biochim Biophys Acta 815:245–258

Maggio B, Albert J, Yu RK (1988) Thermodynamic-geometric correlations for the morphology of self-assembled structures of glycosphingolipids and their mixtures with dipalmitoylphosphatidylcholine. Biochim Biophys Acta 945:145–160. doi:10.1016/0005-2736(88)90477-4

Maggio B, Borioli G a, Del Boca M et al (2008) Composition-driven surface domain structuring mediated by sphingolipids and membrane-active proteins: above the nano- but under the micro-scale: Mesoscopic biochemical/structural cross-talk in biomembranes. Cell Biochem Biophys 50:79–109. doi:10.1007/s12013-007-9004-1

Maggio B, Carrer DC, Fanani ML et al (2004) Interfacial behavior of glycosphingolipids and chemically related sphingolipids. Curr Opin Colloid Interface Sci 8:448–458

Maggio B, Cumar FA, Caputto R (1978) Surface behaviour of Gangliosides and related Glycosphingolipids. Biochem J 171:559–565

Maggio B, Fanani ML, Rosetti CM, Wilke N (2006) Biophysics of sphingolipids II. Glycosphingolipids: an assortment of multiple structural information transducers at the membrane surface. Biochim Biophys Acta Biomembr 1758:1922–1944

Maulik PR, Atkinson D, Shipley GG (1986) X-ray scattering of vesicles of N-acyl sphingomyelins. Determination of bilayer thickness. Biophys J 50:1071–1077. doi:10.1016/S0006-3495(86)83551-2

Merrill AH (2011) Sphingolipid and glycosphingolipid metabolic pathways in the era of sphingolipidomics. Chem Rev 111:6387–6422. doi:10.1021/cr2002917

Niemelä P, Hyvönen MT, Vattulainen I (2004) Structure and dynamics of sphingomyelin bilayer: insight gained through systematic comparison to phosphatidylcholine. Biophys J 87:2976–2989. doi:10.1529/biophysj.104.048702

Pedrera L, Fanani ML, Ros U et al (2014) Sticholysin I-membrane interaction: an interplay between the presence of sphingomyelin and membrane fluidity. Biochim Biophys Acta Biomembr 1838:1752–1759. doi:10.1016/j.bbamem.2014.03.011

Peñalva D a DA, Oresti GMGM, Dupuy F et al (2014a) Atypical surface behavior of ceramides with nonhydroxy and 2-hydroxy very long-chain (C28-C32) PUFAs. Biochim Biophys Acta Biomembr 1838:731–738. doi:10.1016/j.bbamem.2013.11.018

Peñalva D a DA, Wilke N, Maggio B et al (2014b) Surface behavior of sphingomyelins with very long chain polyunsaturated fatty acids and effects of their conversion to ceramides. Langmuir 30:4385–4395. doi:10.1021/la500485x

Peñalva DA, Furland NE, Lopez GH et al (2013) Unique thermal behavior of sphingomyelin species with nonhydroxy and 2-hydroxy very-

long-chain (C28-C32) PUFAs. J Lipid Res 54:2225–2235. doi:10.1194/jlr.M038935

Pinto SN, Silva LC, Futerman AH, Prieto M (2011) Effect of ceramide structure on membrane biophysical properties: the role of acyl chain length and unsaturation. Biochim Biophys Acta Biomembr 1808: 2753–2760. doi:10.1016/j.bbamem.2011.07.023

Poulos a, Johnson DW, Beckman K et al (1987) Occurrence of unusual molecular species of sphingomyelin containing 28-34-carbon polyenoic fatty acids in ram spermatozoa. Biochem J 248:961–964

Poulos a, Sharp P, Johnson D et al (1986) The occurrence of polyenoic fatty acids with greater than 22 carbon atoms in mammalian spermatozoa. Biochem J 240:891–895

Ramstedt B, Slotte JP (1999) Interaction of cholesterol with sphingomyelins and acyl-chain-matched phosphatidylcholines: a comparative study of the effect of the chain length. Biophys J 76: 908–915. doi:10.1016/S0006-3495(99)77254-1

Robinson BS, Johnson DW, Poulos A (1992) Novel molecular species of sphingomyelin containing 2-hydroxylated polyenoic very-long-chain fatty acids in mammalian testes and spermatozoa. J Biol Chem 267:1746–1751

Sandhoff R (2010) Very long chain sphingolipids: tissue expression, function and synthesis. FEBS Lett 584:1907–1913. doi:10.1016/j.febslet.2009.12.032

Shah J, Atienza JM, Duclos RI et al (1995a) Structural and thermotropic properties of synthetic C16:0 (palmitoyl) ceramide: effect of hydration. J Lipid Res 36:1936–1944

Shah J, Atienza JM, Rawlings a V, Shipley GG (1995b) Physical properties of ceramides: effect of fatty acid hydroxylation. J Lipid Res 36:1945–1955

Silvius JR (1992) Cholesterol modulation of lipid intermixing in phospholipid and glycosphingolipid mixtures. Evaluation using fluorescent lipid probes and brominated lipid quenchers. Biochemistry 31: 3398–3408. doi:10.1021/bi00128a014

Silvius JR, Del Giudice D, Lafleur M (1996) Cholesterol at different bilayer concentrations can promote or antagonize lateral segregation of phospholipids of differing acyl chain length. Biochemistry 35: 15198–15208. doi:10.1021/bi9615506

Smaby JM, Kulkarni VS, Momsen M, Brown RE (1996) The interfacial elastic packing interactions of galactosylceramides, sphingomyelins, and phosphatidylcholines. Biophys J 70:868–877. doi:10.1016/S0006-3495(96)79629-7

Smaby JM, Muderhwa JM, Brockman HL (1994) Is lateral phase separation required for fatty acid to stimulate lipases in a phosphatidylcholine interface? Biochemistry 33:1915–1922

Snyder B, Freire E (1980) Compositional domain structure in phosphatidylcholine-cholesterol and sphingomyelin-cholesterol bilayers. Proc Natl Acad Sci U S A 77:4055–4059. doi:10.1073/pnas.77.7.4055

Sot J, Aranda FJ, Collado M-I et al (2005a) Different effects of long- and short-chain ceramides on the gel-fluid and lamellar-hexagonal transitions of phospholipids: a calorimetric, NMR, and x-ray diffraction study. Biophys J 88:3368–3380. doi:10.1529/biophysj.104.057851

Sot J, Goñi FM, Alonso A (2005b) Molecular associations and surface-active properties of short- and long-N-acyl chain ceramides. Biochim Biophys Acta Biomembr 1711:12–19. doi:10.1016/j.bbamem.2005.02.014

Sripada PK, Maulik PR, Hamilton J a, Shipley GG (1987) Partial synthesis and properties of a series of N-acyl sphingomyelins. J Lipid Res 28:710–718

Stults CLM, Sweely CC, Macher BA (1989) Glucosphingolipids: Strucutre, biological source, sand properties. Methods Enzymol 179:167–214

Tettamanti G, Bassi R, Viani P, Riboni L (2003) Salvage pathways in glycosphingolipid metabolism. Biochimie 85:423–437. doi:10.1016/S0300-9084(03)00047-6

Venkataraman K, Futerman AH (2000) Ceramide as a second messenger: sticky solutions to sticky problems. Trends Cell Biol 10:408–412. doi:10.1016/S0962-8924(00)01830-4

Westerlund B, Grandell PM, Isaksson YJE, Slotte JP (2010) Ceramide acyl chain length markedly influences miscibility with palmitoyl sphingomyelin in bilayer membranes. Eur Biophys J 39:1117–1128. doi:10.1007/s00249-009-0562-6

Zanetti SR, Monclus MDLÁ, Rensetti DE et al (2010) Differential involvement of rat sperm choline glycerophospholipids and sphingomyelin in capacitation and the acrosomal reaction. Biochimie 92:1886–1894. doi:10.1016/j.biochi.2010.08.015

Zheng W, Kollmeyer J, Symolon H et al (2006) Ceramides and other bioactive sphingolipid backbones in health and disease: Lipidomic analysis, metabolism and roles in membrane structure, dynamics, signaling and autophagy. Biochim Biophys Acta Biomembr 1758: 1864–1884. doi:10.1016/j.bbamem.2006.08.009